P4.9 A MULTI-PLATFORM SATELLITE TROPICAL CYCLONE WIND ANALYSIS SYSTEM

John A. Knaff *
CIRA/CSU, Fort Collins, CO
and
Mark DeMaria
NOAA/NESDIS, Fort Collins, CO

1. INTRODUCTION

Many new techniques and technologies have been developed in the last decade or so to estimate ocean wind vectors and surface wind speeds from earth orbiting satellites. Examples include passive microwave sensors on Special Sensor Microwave Imager (SSM/I), and WINDSAT, active microwave or scatterometry (i.e., Quikscat, ERS-2, and N-scat), AMSU non-linear balance winds (Bessho et al. 2005), and high resolution low-level feature tracked winds from geostationary satellites (e.g, Holmlund et al. 2001, and Velden et al. 1997). Despite theses advances and the real-time availability of such datasets, there have been relatively few attempts to create a combined wind analysis in and around tropical cyclones.

Detailed tropical cyclone surface wind analyses, until recently, were only possible when aircraft reconnaissance data were available. Such analyses were constructed using H*Wind (i.e., Powell and Houston 1996, and Powell et al. 1996). The H*wind analysis uses a combination of all available surface and near surface wind observations (i.e., satellite based, surface, ships, buoys, aircraft flight level, stepped frequency microwave radiometer, etc.) adjusts them to a common elevation and exposure to create a tropical cyclone wind field. One of the shortcomings of the H*wind analysis system is that it requires a human operator to do some of the quality control of the input data, which makes it difficult to use in the already stressful operational settings.

H*Wind analyses have nonetheless been invaluable in operational, insurance risk assessment and hurricane research communities. However, there availability is limited by 1) the need for a skilled operator and 2) the reliance on aircraft reconnaissance data. As a result, the majority of the world cannot take advantage of such analyses.

* Corresponding Author: John Knaff, CIRA, Colorado State University, Fort Collins, CO 80526; Knaff@cira.colostate.edu

The reliance on aircraft reconnaissance data to generate tropical cyclone wind analyses has been due to the general lack of methods to estimate the very strong winds within a 200 km of the tropical cyclone center. Without methods to estimate the inner region winds, accurate and realistic tropical cyclone wind analyses are not possible. Recent work, however, has led to a couple of techniques that can make estimates of flight-level wind analyses from infrared satellite data (Mueller et al. 2005, Kossin et al. 2006). With the addition of these new techniques, it is now possible to create tropical cyclone wind analyses globally (i.e., wherever infrared imagery is available). In addition, these techniques also make it possible to create satellite only tropical cyclone wind analyses.

With these new methods to estimate tropical cyclone winds within 200km of the cyclone center in hand, the purpose of this paper is to discuss the development of an automated, objective, tropical cyclone surface wind analyses that makes use of these new techniques. While such an analysis could make use of all available wind datasets like H*wind does, the authors want to demonstrate that the estimation of a satellite-only surface wind fields is possible. Sections will include datasets and data treatment, the automated objective analysis system, some examples run in real-time during 2005 and finally the observed shortcomings of the current analysis scheme and plans for improvements.

2. DATASETS AND DATA TREATMENT

Datasets for this satellite-only demonstration include surface wind vector estimates from Quikscat, surface wind speed estimates from SSM/I, feature track winds collected below 500 hPa, 2-d AMSU-based winds (i.e., from solving the 2-d non-linear balance equations as described in Bessho et al. (2005)), and 700-hPa winds derived from IR imagery as described in Mueller et al. (2006). Each of these datasets has its own characteristics and shortcomings. In this section, each of these data types and how

they are combined to form a single flight-level dataset is discussed. The resulting dataset is the input for an analysis.

All of the datasets used are treated in a storm relative manner and are relocated using the storm motion vector to a common analysis time. All datasets are collected in this manner for a 12-h period prior to the analysis, except for the AMSU winds. AMSU 2-d winds are used for a 36-h period because they provide continuity on in the outer regions of the storm. However, these winds receive less weighting if they are older than 12 hours.

Two of the datasets SSM/I and Quikscat are surface observations (i.e., 10-m marine exposure, 1-minute etc.), but most of the other datasets used in this study are in the lower atmosphere. For this reason Quickscat and SSM/I data are adjusted to flight-level (~ 700 hPa) by increasing the wind speed by a factor 0.25 (i.e., divided by 80%) and are rotated 20 degrees toward high pressure.

Quikscat is a k-band (13.4 GHz) radar that senses ocean roughness. The rougher the ocean surface is the greater the wind speed estimate. Two beams are 6 degrees apart that allow for the determination of wind directions. Because of the frequency Quikscat has difficulties determining wind direction in heavy precipitation and high wind speed regimes like the tropical cyclone. For this reason, only wind speeds are analyzed within a 250 km of the tropical storm center. At radii greater than 250 both speed and direction are used.

SSM/I wind speeds, which are based on an algorithm described in Goodberlet et al (1989), have been around for a long time. The algorithm is based on brightness temperatures at 19 GHz (v), 22 GHz (v) and 37GHz (v,h), where v is the vertical polarization and h is the horizontal polarization. These winds are flagged for rain contamination and only unflagged values are used in the tropical cyclone analysis. These winds provide an anchor to the analysis in the environment of the tropical cyclone.

Feature track winds from geostationary satellites are also utilized at pressure levels below 500 hPa. These winds are provided by two agencies via ftp; NRL, Monterey which provides wind fields from international agencies (JMA, BOM, and EU METSAT), and NESDIS who creates winds in the Eastern Pacific and Atlantic basin. These winds are treated as being at one uniform pressure level in the analysis. These winds are primarily located in the region surrounding the tropical cyclone because features that are tracked are typically at levels above 500 hPa near the center of the cyclone. These winds are also useful for anchoring the storm to the environment.

AMSU soundings are utilized to create a two dimensional height field from which wind fields can be calculated by solving the non-linear balance equation. Special processing methods have been developed for creating AMSU-based temperature profiles and height fields as described in Demuth et al. (2004). These height fields were then used to create 2-d wind fields around tropical cyclones as described in Bessho et al. (2005). These winds are created when the center of the AMSU swath is within 700 km of the tropical cyclone's location. Temporal coverage is typically once to four times a day. An example of this type of wind field for the case of Hurricane Ivan on12 September 2004 at 1214 UTC is shown in Fig. 1. Notice that because of the AMSU instruments resolution (~50 km at Nadir), the winds within 100 km of the storm center are poorly estimated. As a result AMSU-based wind vectors are not used within 100 km of the storm center. These data are useful for determining the environment surrounding the storm as well as the near storm asymmetries within the tropical cyclone vortex. Because of their importance to the analysis and because they are less frequent than other data used in the analysis, the AMSU winds are allowed to come into the analysis if they are less than 36 hours old, but only the most recent analysis is used and data older than 12 hours is weighted less (20% less).

The winds in the inner region of the tropical cyclone are estimated from infrared satellite imagery using a method described in Mueller et al. (2005). The technique was developed on 10 years of coincident aircraft and IR imagery. Aircraft data was binned in a storm relative manner over a 12 hour period and analyzed using a variation technique in a cylindrical framework. IR data comes from the automated ingest procedure developed to update a tropical cyclone satellite archive maintained at the Cooperative Institute for Research in the Atmosphere (Zehr 2000). The method predicts the radius of maximum winds and wind speed at 182 km from the center given the storm intensity, location, and the IR imagery. From these parameters a modified Rankine vortex is fit. Asymmetries are added to this 1-d wind field using the storm motion. More complete details of this methodology are provided in Mueller et al (2005). While this technique is

currently being used, an alternative technique described in Kossin et al. (2006) that utilizes the same datasets could also be used in these analyses.

Finally, to maintain continuity from one analysis to the next, the previous analysis is added to the datasets discussed.

Table 1 summarizes the datasets used in this study.

Table 1. A summary of datasets used for making satellite-only tropical cyclone surface wind analyses.

Data type
Tropical cyclone inner winds estimated from Infrared Satellite information
Winds estimated by solving the Non-linear balance equations on AMSU-based Geopotential fields at 850 and 700 hPa
Quikscat surface wind vectors
SSMI-based wind speeds
Water vapor feature tracked winds below 500 hPa
Cloud drift winds (IR and Vis) below 500 hPa
Previous analysis if available

3. ANALYSIS METHODOLOGY

The next step is to perform a preliminary objective wind analysis. The objective analysis is based upon the model-fitting approach with smoothness constraints described by Thacker (1988). In this approach, the difference between the data and the model counterpart of the data is minimized, where the model is simply the wind components on an evenly spaced grid. The model counterpart of the observations is a bilinear interpolation of the wind components to the location of the observation. The smoothness constraints help to fill in the data void areas of the analysis domain.

As an example, suppose there are K observations of a wind components u and v, denoted by u_k and v_k, and M observations of wind speed, denoted by s_m located at arbitrary locations with a domain $x \in [0,L_x]$, $y \in [0,L_y]$. For the objective analysis, the values of u,v and s on an evenly spaced x,y grid with grid spacing of Δx, Δy (denoted by U_{ij}) are determined by minimizing the cost function C defined by

$$C = \frac{1}{2}\sum_{k=1}^{K} w_k \left[(u_k - U_k)^2 + (v_k - V_k)^2 \right] + \sum_{m=1}^{M} w_m (s_m - S_m)^2 + \sum_{i=1}^{I}\sum_{j=1}^{J} \left\{ \begin{array}{l} \alpha\left[(\delta_{xx}U_{ij})^2 + (\delta_{xx}V_{ij})^2\right] \\ + \beta\left[(\delta_{yy}U_{ij})^2 + (\delta_{yy}V_{ij})^2\right] \end{array} \right\} \quad (1)$$

,where δ_{xx} and δ_{yy} are the discretized second derivative operators where

$$\delta_{xx}U_{ij} = (U_{i+1,j} + U_{i-1,j} - 2U_{ij})/\Delta x^2,$$

and

$$\delta_{yy}V_{ij} = (V_{i+1,j} + V_{i-1,j} - 2V_{ij})/\Delta y^2,$$

respectively. In (1) U_k and V_k are the component wind values bi-linearly interpolated from the analysis grid to the observation point k, w_k are data weights, α and β are smoothness parameters, and I and J are the number of analysis points in the x and y directions. Similarly, S_m are the wind speed values interpolated to the observation point m, w_m are the data weights for the wind speed. The first two terms on the right side of (1) measures the misfit between the analysis and the observations and the second term is a constraint that acts as a low-pass filter. As shown by DeMaria and Jones (1994) for the one-dimensional case, the filter response function F(k) for the constraint term in (1) can be written as

$$F(k) = 1/\{1 + 8\alpha[1 - \cos(k\Delta x)]^2\}, \quad (2)$$

where F(k) is the amplitude reduction factor of a pure cosine wave with wavenumber k. Because α is in the denominator in (3) it controls the amount of smoothing. For example, for the $2\Delta x$ wave on the analysis grid ($k=2\pi/2\Delta x$), the amplitude will be reduced by a factor of $(1+32\alpha)^{-1}$. Thus, α and β can be chosen to be consistent with the data coverage relative to the analysis grid spacing. In the analysis code, the fields U_{ij},V_{ij} and S_{ij} that minimized C is found using a simple steepest descent algorithm, which requires the calculation of the gradient of C with respect to U_{ij} and V_{ij} . Given the simple form of (1), the gradient is calculated using an analytic formula.

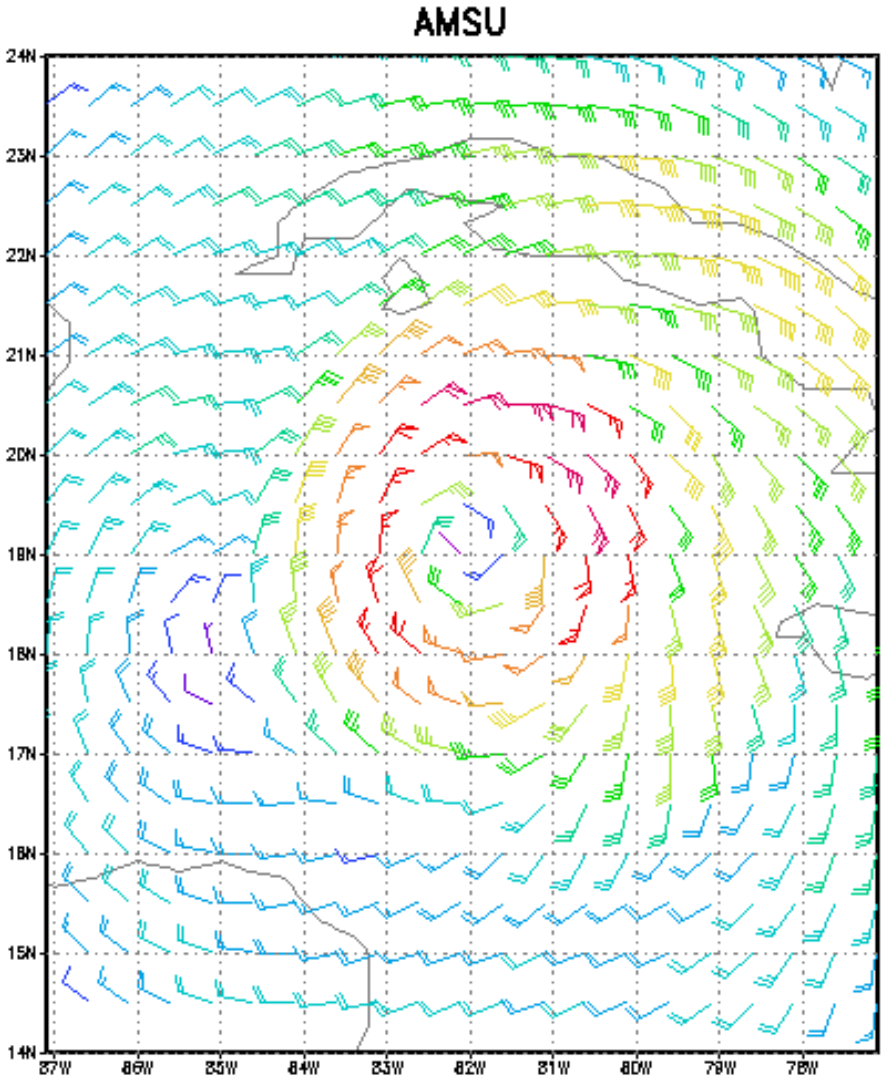

Figure 1. The solution of the non-linear balance equations from 850 hPa geopotential heights estimated from the AMSU soundings for the case of Hurricane Ivan 1214 UTC on 12 September 2004. At this time Hurricane Ivan had estimated maximum 1-minute sustained winds of 135 kt.

For this study, the objective analysis is formulated in cylindrical coordinates with 200 radial points (Δr=4.5 km) from r=2 to 902 km and 36 azimuthal points ($\Delta\theta$=10^o), and the wind components are input as radial and tangential values. An advantage of the cylindrical system is that different smoothness constraints can be applied in the radial and tangential directions. For the analysis, α and β were chose so that the half power wavelengths of the filter were 22.5 km in radius and 100^o in azimuth within 300 km of the center, becoming equally weighted (~350 km) when 500 km or greater from the center.

Different weights (i.e., w_k, w_m) are also applied to the datasets. Figure 2 shows the weights applied to these data as a function of radius. Notice that IR winds have the largest weighting near the center of the storm and the weights on other dataset increase gradually as the distance from the storm center increases.

Analyses are created automatically every 6 hours at 00, 06, 12 and 18 UTC for any storm of tropical depression strength or greater. The

storm location (past and present), and intensity databases are maintained by the Automated Tropical Cyclone Forecast (ATCF) system (Sampson and Schrader 2000). These databases are updated and maintained by the National Hurricane Center (NHC) for the Atlantic and East Pacific, the Central Pacific Hurricane Center for the Central Pacific and the Joint Typhoon Warning Center (JTWC) for the Western North Pacific, North Indian Ocean and Southern Hemisphere.

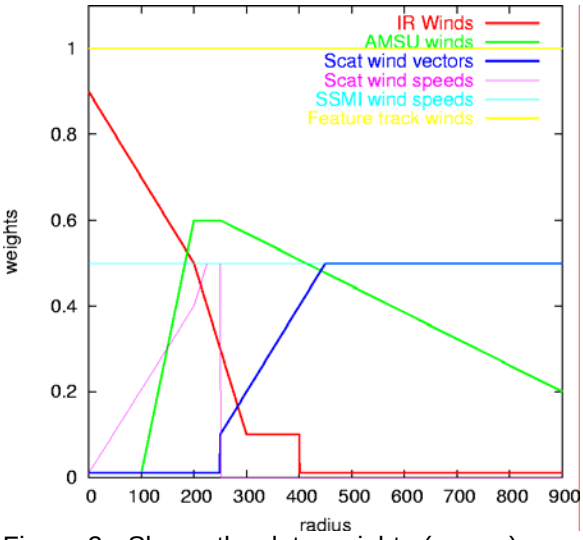

Figure 2. Shows the data weights (w_k, w_m) as a function of radius [km]. Thicker lines are for vector datasets and thinner lines for speed-only datasets. Colors indicate specific datasets as given in the legend. Yellow is feature tracked winds.

Once the various satellite wind data are analyzed to a common level (at ~700 hPa), a marine exposure surface wind reduction is applied. The percent reduction is assumed to be 90% within 150 km and it decrease linearly to 70% at 450 km based partially on Franklin et al. (2003). The winds are turned toward low pressure by 20%. Furthermore a land mask is used to determine if the observation is over land. If the wind observation is over land an additional reduction of 80% is applied and the winds are turned a total of 40% following Boose, et al. (2001).

These efforts result is Satellite-only surface wind analyses for all global tropical cyclones. Examples of these are shown in the next section.

4. EXAMPLE ANALYSES FROM 2005

The 2005 hurricane and typhoon seasons have offered a plethora of cases from which to test a multi-platform satellite tropical cyclone wind analysis. To show the potential usefulness of these wind analyses, the operational estimates of significant wind radii will be compared to those of these analyses for one case. Significant wind radii include the maximum radius of 34-knot, 50-knot and 64-knot winds within quadrants (i.e., northeast, southeast, southwest and northwest) around the storm. The one case we examine is Hurricane Wilma 2005. This is a good case to study such satellite analyses since the Wilma case has aircraft reconnaissance data available for validation for much of its life time and the wind radii estimates are likely more certain.

Hurricane Wilma formed on 15 October in the western Caribbean. It developed into a Category 5 hurricane that set the lowest MSLP for the Atlantic basin early on 19 September. It then hit the Yucatan Peninsula near Cancun late on the 21st and tracked into the Gulf of Mexico and headed toward Florida where it made landfall as a strong Category 3 storm on 24 October. After making landfall in Florida, the storm shot north northwest very quickly and became extratropical on 26 October.

Figure 3 shows the 00 UTC analyses of this storm starting on 17 October and going through 26 October. There are several aspects of the analyses that are important to point out. The first is that these analyses were created in real-time and in doing so some assumptions were made about the future intensity. Since the analyses are created at the synoptic time the official intensity/position estimate is not available. In place of the official intensity/position estimate the previous estimate along with the forecast intensity/position from that time are used. These assumptions were used to create not only these analyses but the IR-based winds. As a result during the period of rapid intensification from the 18th to 19th of October, the maximum winds in these analyses are underestimated. Despite the resulting wind and position errors, the analysis is still able to capture somewhat realistic radii of maximum winds and wind radii (shown in the bottom text of each figure).

The realistic expansion of the wind radii in these analyses are shown in Figure 4, which compares the official wind radii estimates from NHC to those estimated in the satellite only

analyses. Notice that the wind radii follow common trends in all the significant wind radii estimates. This is noteworthy as Wilma had rather small wind radii initially, but grew to have relatively large wind radii later.

For a better idea of how these estimates compare, Table 2 shows a quantitative comparison between the NHC wind radii and those estimated by the satellite only wind analysis. Notice that the analyses for Wilma have positive biases for the estimates of 34, and 50-kt winds. The mean absolute errors (MAE) are about 47 nm, 27 nm, and 15 nm for the 34, 50 and 64-kt wind radii estimates in all quadrants. The RMS errors are quite a bit larger due to the rather systematic positive bias in the 34 and 50-kt wind radii. The estimates of 64-kt winds are encouraging given the fact that these winds are being estimated primarily by the IR technique discussed in Mueller et al. (2005)

Table 2. Quantitative comparison between NHC's estimates of radii of 34, 50 and 64-kt winds and similar estimates made using a satellite-only surface wind analysis. Units are in nautical miles and the number of cases is given for each radii.

34-kt wind radii, N=35				
	NE	**SE**	**SW**	**NW**
Biases	26.8	30.0	26.2	10.0
MAE	50.4	55.8	43.9	40.7
RMSE	65.3	70.1	55.8	52.9
50-kt wind radii, N=32				
	NE	**SE**	**SW**	**NW**
Biases	9.8	12.4	26.9	-1.9
MAE	27.0	30.4	32.0	16.5
RMSE	39.5	49.5	60.8	21.8
64-kt wind radii, N=30				
	NE	**SE**	**SW**	**NW**
Biases	-3.6	2.9	1.3	-6.1
MAE	15.8	17.3	12.0	16.0
RMSE	19.9	23.4	19.9	20.6

Results presented in this section suggest that a satellite only surface wind analysis may be useful for estimating the wind fields associated with tropical cyclones. This will allow for better estimation of significant wind radii in cases when aircraft reconnaissance data is unavailable - which is most of the world's tropical cyclone cases. Furthermore, such analyses could be used for other purposes (i.e., wave model initialization, risk modeling, etc.). However, as is often the case, there are a few shortcomings with this analysis method which will be discussed briefly in the next section.

5. ANALYSIS SHORTCOMING AND FUTURE PLANS

The analyses presented have a strong dependency on the AMSU-based winds. When these winds are not available the region located between 200km and 400 km from the cyclone center has very few reliable data observations. To correct this shortcoming an attempt to make the filter parameters and data weights a function of the datasets available, and the number of points available to analyze is planned.

In addition, rapidly accelerating storms seem to create problems with the handling of the storm relative input data, especially those of the AMSU-based data when they are more than 12-hours old. This will likely continue to be a problem.

Another problem is the biases observed in this case study. A larger validation sample is needed to determine if these biases are systematic. Once such systematic biases are determined the surface model will be adjusted accordingly. Such an evaluation is planned.

Some of the errors associated with these analyses may be reduced by the incorporation of inner core wind vectors created using the methodology described by Kossin et al. (2006), which does not rely on a parametric vortex model. The use of winds created using this methodology is also planned in the near future.

Once the biases and data issues are resolved, this product will hopefully be considered for a transition from its current experimental state to an operational product. Such a product could be produced for all globally occurring tropical cyclones where it could be used for model initialization, research studies, and generation of operational products.

Acknowledgements: This work was funded by *NOAA grant NA17RJ1228* as part of a project to create a satellite-only tropical cyclone surface wind analysis. The authors would also like to thank Buck Sampson at NRL, Monterey for real-time access to cloud track winds and Stan Kidder of CIRA for real-time access to SSM/I wind speed estimates.

The views, opinions, and findings in this report are those of the authors and should not be construed as an official NOAA and or U.S. Government position, policy, or decision.

References:

Bessho, K. M. DeMaria, J. A. Knaff, 2005: Tropical Cyclone Wind Retrievals from the Advanced Microwave Sounder Unit (AMSU): Application to Surface Wind Analysis., J. App. Met, in press.

Boose, E. R., K. E. Chamberland, D. R. Foster, 2001: Landscape and regional impacts of hurricanes in New England. Ecological Monographs, 71:**1**, 27-48.

DeMaria, M., and R.W. Jones, 1993: Optimization of a hurricane track forecast model with the adjoint model equations. *Mon. Wea. Rev.*, **121**, 1730-1745.

Franklin, J. L. , M.L. Black, and K. Valde, 2003: GPS dropwindsonde wind profiles in hurricanes and their operational implications. Wea. Forecasting, 18:**1**, 32-44.

Goodberlet, M. A., Swift, C. T. and Wilkerson, J. C., Remote Sensing of Ocean Surface Winds With the Special Sensor Microwave/Imager, J. Geophys. Res.,**94**, 14574-14555, 1989

Graf, J.E.; Wu-yang Tsi; Jones, L., 1998: Overview of QuikSCAT mission-a quick deployment of a high resolution, wide swath scanning scatterometer for ocean wind measurement, Proceedings. IEEE Southeastcon '98. `Engineering for a New Era' (Cat. No.98CH36170), p. xiv+416, 314-17

Holmlund K., C. S. Velden and M. Rohn, 2001: Enhanced Automated Quality Control Applied to High-Density Satellite-Derived Winds. *Mon. Wea. Rev.*,129:**3**, 517–529.

Kossin, J. P., J. A. Knaff, T. A. Cram, and H. Berger, 2006: Estimating Inner-Core Hurricane Structure in the Absence of Aircraft Reconnaissance. In preparation for *Mon. Wea. Rev.*

Mueller, K. J., M. DeMaria, J. A. Knaff, J. P. Kossin, and T. H. VonderHaar, 2005: Objective Estimation of Tropical Cyclone Wind Structure from Infrared Satellite Data, Accepted pending revisions to *Wea. Forecasting.*

Powell, M. D., and S. H. Houston, 1996: Hurricane Andrew's landfall in south Florida. Part II: Surface wind fields and potential real-time applications. *Wea. Forecasting,* **11,** 329–349.

____, S. H. Houston, and T. Reinhold, 1996: Hurricane Andrew's landfall in south Florida. Part I: Standardizing measurements for documentation of surface wind fields. *Wea. Forecasting,* **11,** 304–328.

Sampson, C. R. and A. J. Schrader, 2000: The automated tropical cyclone forecasting system (Version 3.2). *Bull. Amer. Met. Soc*., **81**, 1231-1240.

Thacker, W. C., 1988: Fitting models to inadequate data by enforcing spatial and temporal smoothing. *J. Geophys. Res.,* **93**, 10655–10665.

Velden C. S., C. M. Hayden, S. J. Nieman, W. P. Menzel, S. Wanzong and J. S. Goerss. 1997: Upper-Tropospheric Winds Derived from Geostationary Satellite Water Vapor Observations. *Bull. Amer. Met. Soc.*, 78:**2**, 173–195.

Zehr, R.M., 2000: Tropical cyclone research using large infrared image data sets. *24th Conference on Hurricanes and Tropical Meteorology*. 29 May - 2 June, Fort Lauderdale, FL, Amer. Meteor. Soc., 486-487.

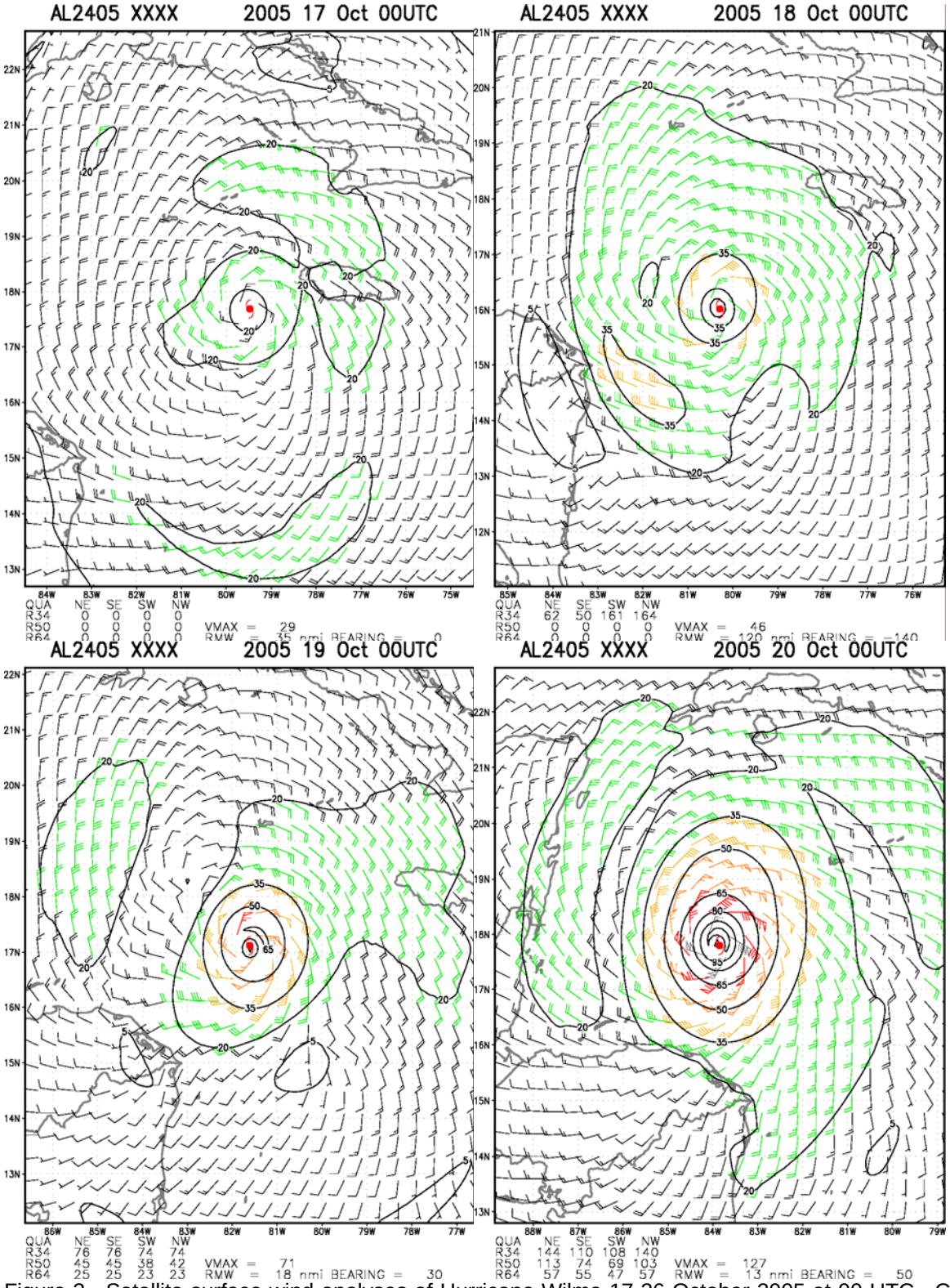

Figure 3. Satellite surface wind analyses of Hurricane Wilma 17-26 October 2005 at 00 UTC. Contours start at 20 and have increments of 15 kt.

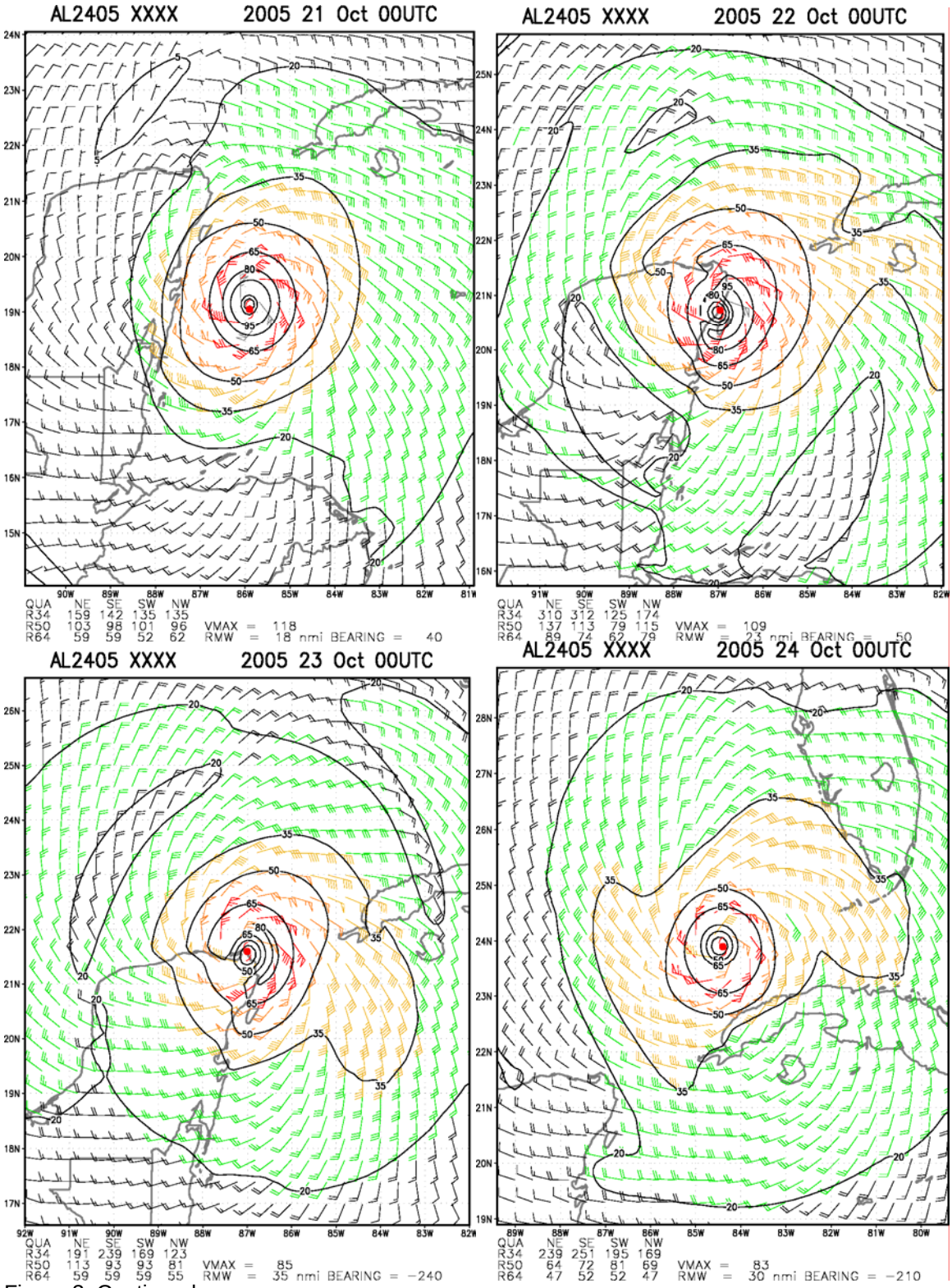

Figure 3. Continued.

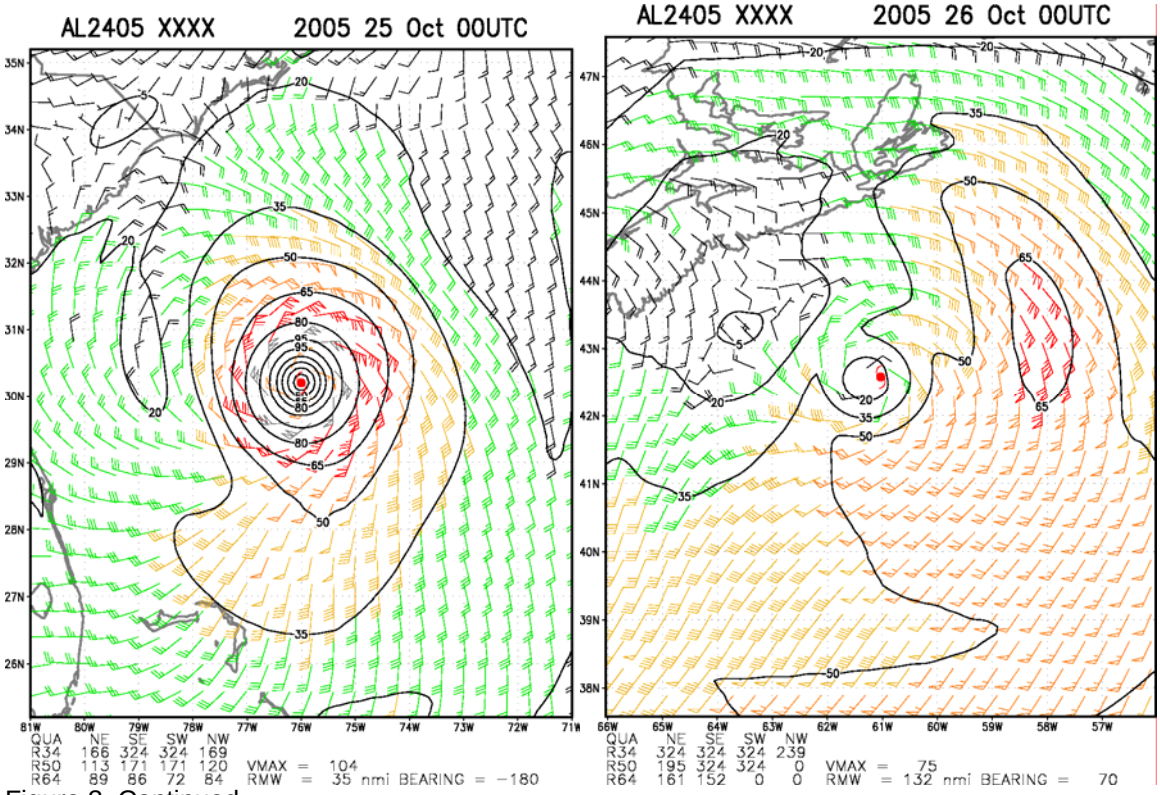

Figure 3. Continued.

Figure 4. Comparisons of time series of significant wind radii estimated at NHC to those estimated from the satellite-only surface wind analysis. Shown are 4 panels for each quadrant (NE,SE,SW,NW) of the storm. These panels are orientated so that the top of the page is north. The first set of panels shows the comparison of the radius of 34-kt winds. This is followed by the 50-kt wind radii and the 64-kt wind radii.

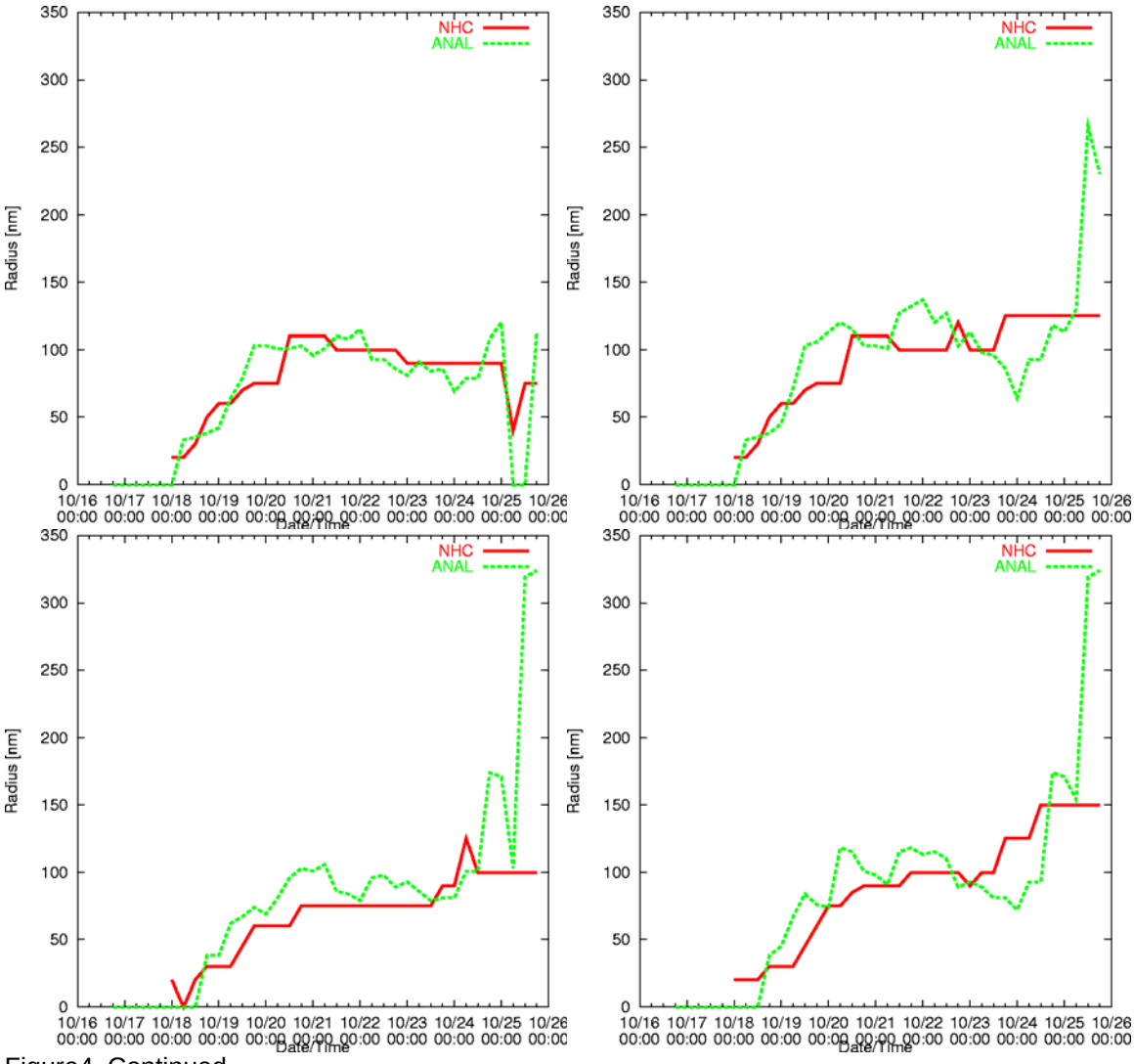

Figure4. Continued.

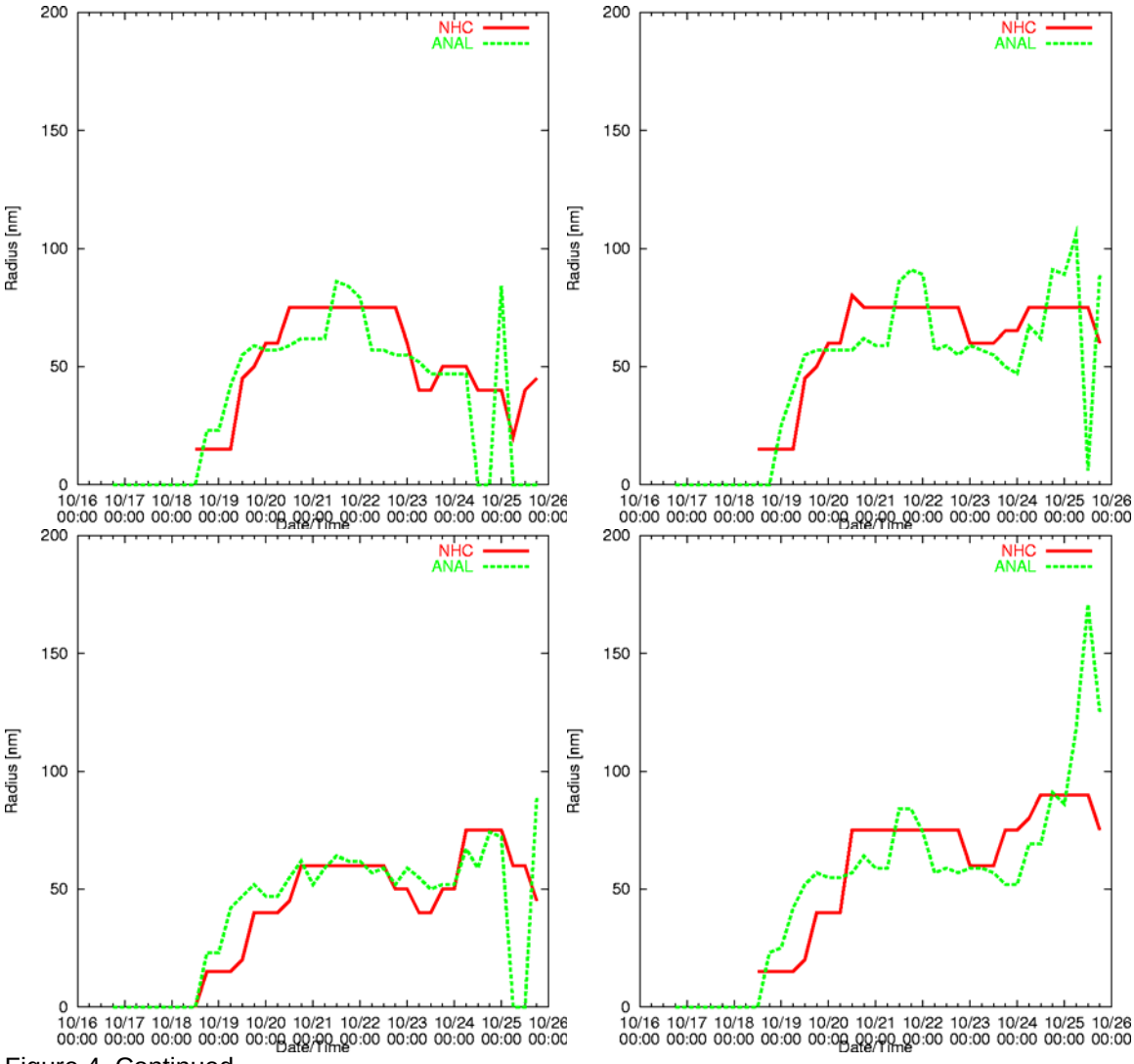

Figure 4. Continued.